Solving characteristic equation of orbital angular momentum modes in a ring fiber

Yixiao Zhu (朱逸萧) and Fan Zhang (张 帆)*

State Key Laboratory of Advanced Optical Communication Systems and Networks, Peking University, Beijing 100871, China

**Corresponding author: fzhang@pku.edu.cn*

Received October 8, 2014; accepted December 22, 2014; posted online March 12, 2015

The characteristic equation of orbital angular momentum modes in a ring fiber is derived. By solving the equation with the graphical method, mode distribution in a ring fiber can be precisely determined for arbitrary fiber parameters without relying on simulation of the vector field. This will provide a useful method to determine the separation between quasi-degenerate modes in a ring fiber.

OCIS codes: 050.4865, 060.2270, 060.2310.

doi: 10.3788/COL201513.030501.

Light beams carrying orbital angular momentum (OAM) are characterized as a spiral phase structure of $\exp(\mathrm{i}l\theta)$, where l is topological charge (an integer), and θ is the azimuthal angle[1,2]. The OAM modes with different topological charge number l are inherently orthogonal to each other, and therefore can be considered as an additional available degree of freedom for multiplexing information[1,3]. Combining OAM with other traditional multiplexing technologies such as wavelength division multiplexing (WDM), the capacity and spectral efficiency of optical communication systems will be greatly enhanced[3–5].

Although there have been several reports for free-space transmission based on OAM[3,5,6], transmission in fiber can avoid atmospheric disturbance[7], and make long-distance transmission feasible. However, OAM modes are unstable in terms of propagation in a conventional step-index fiber due to the mode coupling[2,8]. It is known that hybrid modes (HE_{lm} and EH_{lm}) are Eigen modes in a fiber. The combination of quasi-degenerate $\mathrm{HE}_{l+1,m}$ and $\mathrm{EH}_{l-1,m}$ modes results in linearly polarized (LP) modes (i.e., $\mathrm{LP}_{l,m} = \mathrm{HE}_{l+1,m} + \mathrm{EH}_{l-1,m}$, $l \geq 1$), while the combination of intrinsic degenerate $\mathrm{HE}_{lm}^{\mathrm{odd}}$ and $\mathrm{HE}_{lm}^{\mathrm{even}}$ ($\mathrm{EH}_{lm}^{\mathrm{even}}$ and $\mathrm{EH}_{lm}^{\mathrm{even}}$) modes with $\pi/2$ phase shift generates OAM modes [i.e., $\mathrm{OAM}_{\pm(l-1)} = \mathrm{HE}_{lm}^{\mathrm{even}} \pm \mathrm{i} \times \mathrm{HE}_{lm}^{\mathrm{odd}}$, $\mathrm{OAM}_{\pm(l+1)} = \mathrm{EH}_{lm}^{\mathrm{even}} \pm \mathrm{i} \times \mathrm{EH}_{lm}^{\mathrm{odd}}$][8–10]. In a conventional multimode fiber, LP modes are easily produced by coupling because the effective refractive index (ERI) difference between $\mathrm{HE}_{l+1,m}$ and $\mathrm{EH}_{l-1,m}$ modes is too small[2,4,8]. To overcome this problem, several schemes were proposed such as coiling the fiber[11], using spun elliptical and anisotropic fibers[12], and the intensely twisted elliptical fiber was based on band-gap Bragg selection[13]. Nevertheless, recently more attention has been paid to the structure of a ring fiber, which splits the quasi-degenerate modes by increasing the ERI difference. The generation of a higher-order OAM mode in a ring fiber has been studied[14] and analysis of the modes has been given[15]. Then generation and multiplexing OAM modes in a ring fiber was proposed[16]. To our best knowledge, theoretical analysis of the mode properties in a ring fiber made before are all based on the weakly guiding approximation (WGA), which focus on LP modes and thus cannot show the difference between quasi-degenerate modes[17,18].

In this Letter, a modal characteristic equation is derived by rigorously solving the Helmholtz equation. Based on this characteristic equation, we investigate the influence of the ring fiber structure parameters on the ERI of the Eigenmodes. Besides, it should be noted that the exact degeneracy of two optical vortices with opposing topological charges and spin will interact each other due to infinitesimal ellipticity induced by stress[19]. However, our theory is applicable to the ideal ring fiber, and the situation where fibers are slightly elliptical deserves further study.

Figure 1 shows the cross section and the refractive index (RI) profile of a ring fiber. It consists of three concentric regions: the inner clad, the core, and the outer clad. The RI of the core is n_1 while the RI of the inner and outer clad are both n_2 which satisfies $n_1 > n_2$. The inner radius and outer radius of ring fiber are r_1 and r_2, respectively. A cylindrical coordinates is set due to the longitude invariance and the angular symmetry of the geometry. We first deal with the longitudinal components of the electric and magnetic field by solving the Helmholtz equation[20].

$$\nabla^2 \begin{Bmatrix} E_z \\ H_z \end{Bmatrix} + k^2 \begin{Bmatrix} E_z \\ H_z \end{Bmatrix} = 0, \tag{1}$$

where $\nabla^2 = \frac{\partial^2}{\partial r^2} + \frac{1}{r}\frac{\partial}{\partial r} + \frac{1}{r^2}\frac{\partial^2}{\partial \theta^2} + \frac{\partial^2}{\partial z^2}$, and k is the wavenumber in the corresponding regions. By applying the method of variable separation, E_z can be written as

$$E_z = R(r)\exp(\pm \mathrm{i}l\theta)\exp(\mathrm{i}\beta z), \tag{2}$$

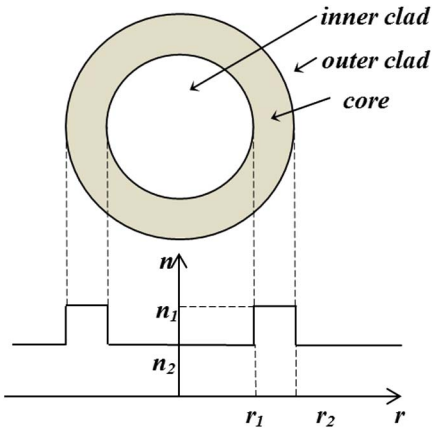

Fig. 1. Cross sectional diagram of a ring fiber.

$$R(r)=\begin{cases} aI_l(vr) & 0\le r<r_1 \\ bJ_l(ur)+cY_l(ur) & r_1\le r<r_2 \\ dK_l(vr) & r_2\le r \end{cases}, \tag{3}$$

$$\begin{aligned} u^2&=n_1^2k_0^2-\beta^2, \\ v^2&=\beta^2-n_2^2k_0^2, \end{aligned} \tag{4}$$

where β is the propagation constant along the z-axis direction, ω is the angular frequency, and k_0 is the wavenumber in vacuum. J_l and Y_l are Bessel functions of the first kind and the second kind, respectively. I_l and K_l denote the modified Bessel functions of the first kind and the second kind, respectively. The subscript l is the order of the Bessel function which is an integer. The terms a, b, c, and d are constants to be determined by boundary conditions. The term of $\exp(\pm \mathrm{i}l\theta)$ in Eq. (2) shows the total angular momentum (AM) of the Eigen modes in the ring fiber, where "±" denotes that each of the modes ($l\ge 1$) has two inherent degeneracies. If $\{\sin(l\theta),\cos(l\theta)\}$ is set as the basis instead of $\{\exp(\mathrm{i}l\theta),\exp(-\mathrm{i}l\theta)\}$ for the angular part in Eq. (2), we can get the odd and the even modes as mentioned previously[9,20,21]. Note that total AM consists of both spin angular momentum (SAM) and OAM[14]. The combination of the odd and even modes with $\pi/2$ phase shift become OAM modes with a total AM of $1\hbar$, where the OAM part is $(l+1)\hbar$ when the SAM is antiparallel with the OAM or $(l-1)\hbar$ when the SAM is parallel with the OAM. The corresponding magnetic field component H_z can be obtained by substituting the constants e, f, g, and h for a, b, c, and d, respectively.

After E_z and H_z were formulized, the rest of the components E_r, E_θ, H_r, and H_θ can be derived from the following relations[20]

$$\begin{cases} E_r=\dfrac{\mathrm{i}\beta}{\omega^2\mu\varepsilon-\beta^2}\left(\dfrac{\partial E_z}{\partial r}+\dfrac{\omega\mu}{\beta r}\dfrac{\partial H_z}{\partial\theta}\right) \\ E_\theta=\dfrac{\mathrm{i}\beta}{\omega^2\mu\varepsilon-\beta^2}\left(-\dfrac{\omega\mu}{\beta}\dfrac{\partial H_z}{\partial r}+\dfrac{1}{r}\dfrac{\partial E_z}{\partial\theta}\right) \\ H_r=\dfrac{\mathrm{i}\beta}{\omega^2\mu\varepsilon-\beta^2}\left(\dfrac{\partial H_z}{\partial r}-\dfrac{\omega\varepsilon}{\beta r}\dfrac{\partial E_z}{\partial\theta}\right) \\ H_\theta=\dfrac{\mathrm{i}\beta}{\omega^2\mu\varepsilon-\beta^2}\left(\dfrac{\omega\varepsilon}{\beta}\dfrac{\partial E_z}{\partial r}+\dfrac{1}{r}\dfrac{\partial H_z}{\partial\theta}\right) \end{cases}, \tag{5}$$

where μ and ε are permeability and permittivity of the corresponding regions, respectively. In our calculation, $\mu=\mu_0$ and $\varepsilon=\varepsilon_0 n^2$ is adopted where μ_0 and ε_0 are respectively permeability and permittivity of vacuum[20].

To determine the eight constants a–h, we apply the continuity conditions of the electromagnetic field components E_z, E_θ, H_z, and H_θ at the interfaces of $r=r_1$ and $r=r_2$ to obtain eight ($=4\times 2$) equations. Then a nonzero solution for the set of equations requires its determinant of coefficient to equal zero[22], which is shown as Eq. (6). By using the Gauss elimination method[22], the 8×8 determinant mentioned previously can be reduced to a 4×4 form of Eq. (7).

$$\begin{vmatrix} I_l(vr_1) & -J_l(ur_1) & -Y_l(ur_1) & 0 & 0 & 0 & 0 & 0 \\ \dfrac{\mathrm{i}l\beta}{v^2r_1}I_l(vr_1) & \dfrac{\mathrm{i}l\beta}{u^2r_1}J_l(ur_1) & \dfrac{\mathrm{i}l\beta}{u^2r_1}Y_l(ur_1) & 0 & \dfrac{\omega\mu}{v}I_1'(vr_1) & \dfrac{\omega\mu}{u}J_1'(ur_1) & \dfrac{\omega\mu}{u}Y_1'(ur_1) & 0 \\ 0 & 0 & 0 & 0 & I_l(vr_1) & -J_l(ur_1) & -Y_l(ur_1) & 0 \\ \dfrac{\omega\varepsilon_2}{v}I_1'(vr_1) & \dfrac{\omega\varepsilon_1}{u}J_1'(ur_1) & \dfrac{\omega\varepsilon_1}{u}Y_1'(ur_1) & 0 & -\dfrac{\mathrm{i}l\beta}{v^2r_1}I_l(vr_1) & -\dfrac{\mathrm{i}l\beta}{u^2r_1}J_l(ur_1) & -\dfrac{\mathrm{i}l\beta}{u^2r_1}Y_l(ur_1) & 0 \\ 0 & J_l(ur_2) & Y_l(ur_2) & -K_l(vr_2) & 0 & 0 & 0 & 0 \\ 0 & \dfrac{\mathrm{i}l\beta}{u^2r_2}J_l(ur_2) & \dfrac{\mathrm{i}l\beta}{u^2r_2}Y_l(ur_2) & \dfrac{\mathrm{i}l\beta}{v^2r_2}K_l(vr_2) & 0 & \dfrac{\omega\mu}{u}J_1'(ur_2) & \dfrac{\omega\mu}{u}Y_1'(ur_2) & \dfrac{\omega\mu}{v}K_1'(vr_2) \\ 0 & 0 & 0 & 0 & 0 & J_l(ur_2) & Y_l(ur_2) & -K_l(vr_2) \\ 0 & \dfrac{\omega\varepsilon_1}{u}J_1'(ur_2) & \dfrac{\omega\varepsilon_1}{u}Y_1'(ur_2) & \dfrac{\omega\varepsilon_2}{v}K_1'(vr_2) & 0 & -\dfrac{\mathrm{i}l\beta}{u^2r_2}J_l(ur_2) & -\dfrac{\mathrm{i}l\beta}{u^2r_2}Y_l(ur_2) & -\dfrac{\mathrm{i}l\beta}{v^2r_2}K_l(vr_2) \end{vmatrix} = 0, \tag{6}$$

$$\begin{vmatrix} \frac{\mathrm{i}l\beta}{\omega\mu r_1}\left(\frac{1}{u^2}+\frac{1}{v^2}\right) & \frac{\mathrm{i}l\beta}{\omega\mu r_1}\left(\frac{1}{u^2}+\frac{1}{v^2}\right) & E & F \\ \varepsilon_0 W & \varepsilon_0 X & -\frac{\mathrm{i}l\beta}{\omega r_1}\left(\frac{1}{u^2}+\frac{1}{v^2}\right) & -\frac{\mathrm{i}l\beta}{\omega r_1}\left(\frac{1}{u^2}+\frac{1}{v^2}\right) \\ \frac{\mathrm{i}l\beta}{\omega\mu r_2}\left(\frac{1}{u^2}+\frac{1}{v^2}\right) & \frac{\mathrm{i}l\beta}{\omega\mu r_2}\left(\frac{1}{u^2}+\frac{1}{v^2}\right) & G & HK \\ \varepsilon_0 Y & \varepsilon_0 ZK & -\frac{\mathrm{i}l\beta}{\omega\mu r_2}\left(\frac{1}{u^2}+\frac{1}{v^2}\right) & -\frac{\mathrm{i}l\beta}{\omega\mu r_2}\left(\frac{1}{u^2}+\frac{1}{v^2}\right)K \end{vmatrix} = 0. \quad (7)$$

Here variable substitution is adopted in the following two steps.

$$\text{Step 1: } A_1 = \frac{I_l'(vr_1)}{I_l(vr_1)}, \quad B_i = \frac{J_l'(ur_i)}{J_l(ur_i)}, \quad C_i = \frac{I_l'(ur_i)}{I_l(ur_i)}, \quad D_2 = \frac{K_l'(vr_2)}{K_l(vr_2)} \quad (i=1,2), \quad (8)$$

$$\begin{aligned} \text{Step 2: } E &= \frac{B_1}{u}+\frac{A_1}{v}, \quad F = \frac{C_1}{u}+\frac{A_1}{v}, \\ G &= \frac{B_2}{u}+\frac{D_2}{v}, \quad H = \frac{C_2}{u}+\frac{D_2}{v}, \\ K &= \frac{Y_l(ur_2)/Y_l(ur_1)}{J_l(ur_2)/J_l(ur_1)} \quad W = \frac{n_1^2 B_1}{u}+\frac{n_2^2 A_1}{v}, \\ X &= \frac{n_1^2 C_1}{u}+\frac{n_2^2 A_1}{v}, \quad Y = \frac{n_1^2 B_2}{u}+\frac{n_2^2 D_2}{v}, \\ Z &= \frac{n_1^2 C_2}{u}+\frac{n_2^2 D_2}{v}, \quad M = \frac{l\beta}{k_0}\left(\frac{1}{u^2}+\frac{1}{v^2}\right). \end{aligned} \quad (9)$$

Finally the characteristic equation of a ring fiber is obtained in Eq. (10) by expanding the determinant.

$$\begin{aligned} &\frac{M^4}{r_1^2 r_2^2}(K-1)^2 + (KEH-FG)(KWZ-XY) \\ &- M^2\left[\frac{(KH-G)(KZ-Y)}{r_1^2}+\frac{(KE-F)(KW-X)}{r_2^2}\right. \\ &\left.- K\frac{(E-F)(Y-Z)+(H-G)(X-W)}{r_1 r_2}\right] = 0. \end{aligned} \quad (10)$$

To go back into the case of the step-index fiber, the first four rows and the first, third, fifth, and seventh column of the last four rows of the determinant in Eq. (6) should be removed. To go back into the case of WGA for the ring fiber, $\beta \approx k_0 n_1 \approx k_0 n_2$ should be adopted in Eq. (10). It means variables in Eqs. (8) and (9) evolving like $W \to n_1^2 E$, $X \to n_1^2 F$, $Y \to n_1^2 G$, and $Z \to n_1^2 H$. These two special cases can be considered as verification of the modal characteristic equation[17–19].

Equation (10) is a complicated transcendental equation with Bessel function contains the propagation constant. We define the left-hand side of Eq. (10) as a function f and study its curve intersection with the x-axis. For we set the structure parameters as $n_1 = 1.5$, $n_2 = 1.45$, $r_1 = 4$ μm, and $r_2 = 5$ μm and obtain the ERI of different modes. Table 1 shows the comparison between the simulation results of the finite element analysis software COMSOL and roots of our mode characteristic equation, where the solution of Eq. (10) fits the simulation results very well with a relative error at the magnitude of 10^{-6} or less.

Then we can use Eqs. (3) to obtain the electric field distribution of them, which is depicted in Fig. 2.

Based on Eq. (10), we can investigate the ERI difference between quasi-degenerate modes. Here we take TE_{01} and HE_{21} as an example so as to compare with the previous work by Yue *et al.*[9,10] Figure 3 shows the influence caused by changing wavelength λ and the RI difference of the fiber core $\Delta n = n_1 - n_2$. The parameters are set fixed as $r_1 = 4$ μm, $r_2 = 5$ μm, and $n_2 = 1.444$. Figure 3 shows that the ERI difference between the quasi-degenerate modes is larger than 10^{-4}, which was proven valid for mode separation and stable transmission of OAM[4,8,21].

Analogously to the step-index fiber, we introduce the normalized propagation constant b, the normalized frequency V, and the average radius of the ring r_{ave} as[20]

$$b = \frac{\beta^2 - k_0 n_2^2}{k_0 n_1^2 - k_0 n_2^2}, \quad (11)$$

$$V^2 = k_0^2 (r_2 - r_1)^2 (n_1^2 - n_2^2), \quad (12)$$

Table 1. Comparison between Simulation Results and the Solution of Eq. (10)

Mode	Simulation Result	Eq. (10) Solution	Relative Error
HE_{11}	1.467350	1.467352	1.4×10^{-6}
TE_{01}	1.466638	1.466641	2.0×10^{-6}
HE_{21}	1.466159	1.466162	2.0×10^{-6}
TM_{01}	1.465566	1.465566	$<10^{-6}$
HE_{31}	1.462827	1.462831	2.7×10^{-6}
EH_{11}	1.462714	1.462715	6.8×10^{-7}
HE_{41}	1.457518	1.457526	5.5×10^{-6}
EH_{21}	1.457473	1.457475	1.4×10^{-6}
EH_{31}	1.450510	1.450517	4.8×10^{-6}

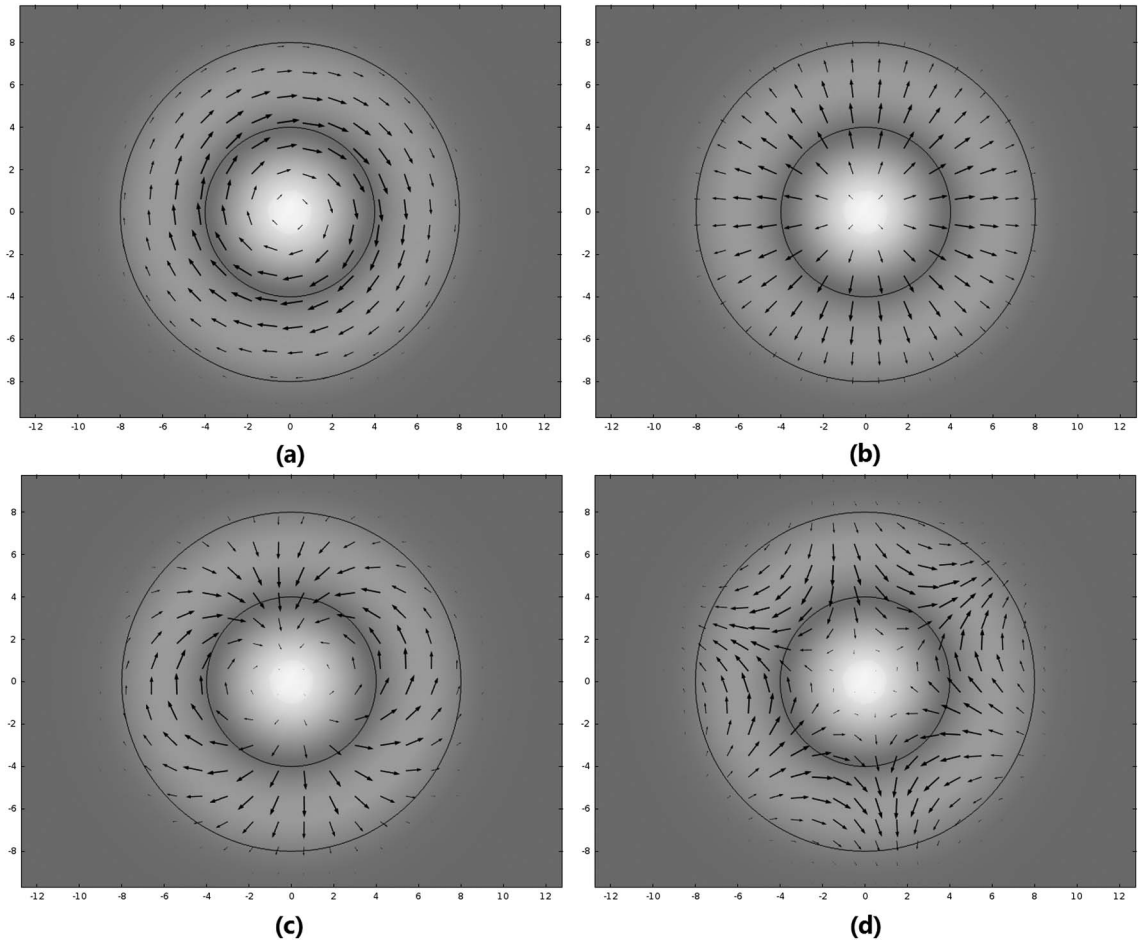

Fig. 2. Electric field distribution on the cross section for several modes; (a) TE_{01}; (b) TM_{01}; (c) EH_{11}; (d) HE_{31}.

$$r_{\text{ave}} = (r_1 + r_2)/2. \tag{13}$$

The term V is determined by structure parameters of the ring fiber. The term b can be regarded as a single-value function of V and r_{ave}, which is of great importance for guiding the structure design of a multimode ring fiber. Figure 4 shows the influence of V and r_{ave} to the b value of HE_{11} mode, in which $r_2 - r_1 = 2$ μm and $n_2 = 1.4$ both remain unchanged. We can find that the HE_{11} mode exhibits a zero cutoff. Figure 5 shows b of the low-order modes in a ring fiber as a function of V with the average radius of the ring is set as 3, 5, 7.5, and 10 μm, respectively. As b is a normalized variable, Fig. 5 illustrates the relative degree of separation among quasi-degenerate modes. The ERI difference of HE_{21} from TE_{01} and TM_{01} achieve 10^{-4}

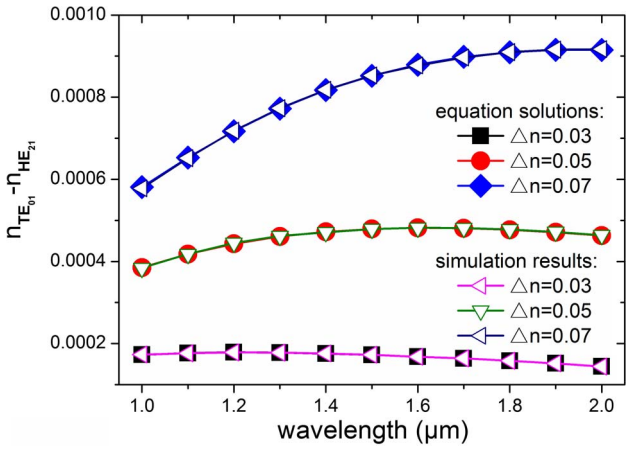

Fig. 3. ERI difference between TE_{01} and HE_{21} as a function of the index difference and the wavelength.

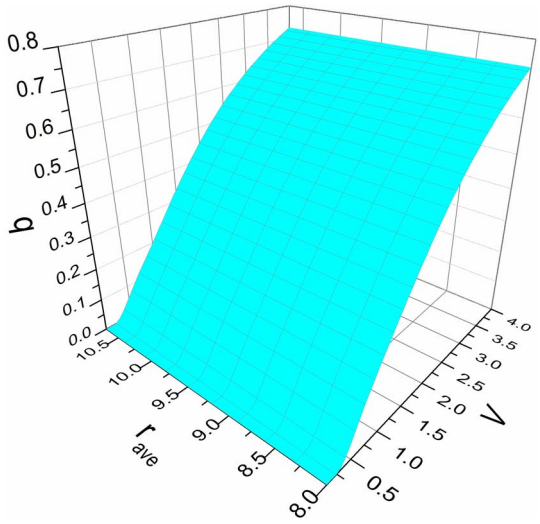

Fig. 4. Normalized propagation constant b for HE_{11} as a function of the normalized frequency V and the average radius of the ring.

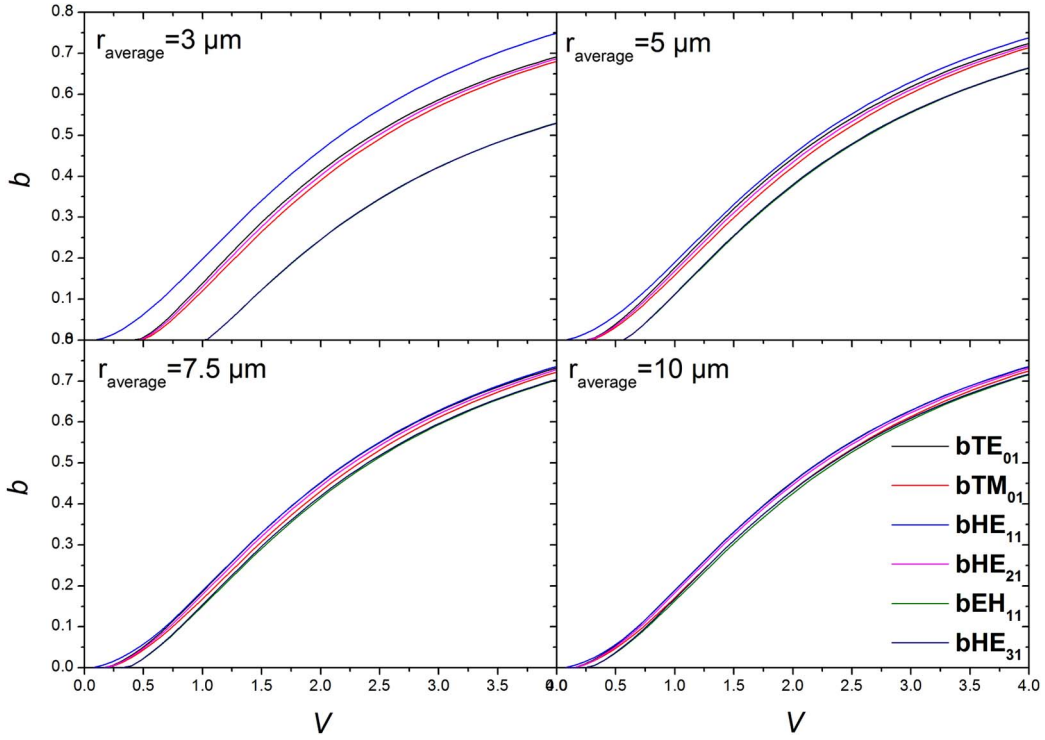

Fig. 5. Normalized propagation constant b of modes in a ring fiber as a function of the normalized frequency V with the average radius of the ring set as 3, 5, 7.5, and 10 μm.

with $n_1 - n_2 = 0.05$ while the separation between EH_{11} and HE_{31} is guaranteed with $n_1 - n_2 = 0.1$. In addition, the cutoff frequency of the modes decreases as the average radius of the ring increases.

In conclusion, we strictly deduce the OAM modal characteristic equation of a ring fiber from the Helmholtz equation. It also points out that our equation can reduce to the conventional cases of a step-index fiber and a ring fiber under the condition of WGA. Furthermore, the mode distributions in a ring fiber can be precisely illustrated for arbitrary fiber parameters without relying on simulation of the vector field.

This work was supported by the National Hi-Tech Research and Development Program of China (No. 2012AA011302) and the National Natural Science Foundation of China (No. 61475004).

References

1. M. Vasnetsov and K. Staliunas, "Optical vortices," in *Horizons of World Physics* (Nova Science, 1999), Vol. **228**.
2. C. N. Alexeyev, A. V. Volyar, and M. A. Yavorsky, "Fiber optical vortices," in *Lasers, Optics and Electro-Optics Research Trends*, L. I. Chen, ed. (Nova, 2007).
3. J. Wang, J.-Y. Yang, I. M. Fazal, N. Ahmed, Y. Yan, H. Huang, Y. Ren, Y. Yue, S. Dolinar, M. Tur, and A. E. Willner, Nat. Photonics **6**, 488 (2012).
4. N. Bozinovic, Y. Yue, Y. Ren, M. Tur, P. Kristensen, H. Huang, A. E. Willner, and S. Ramachandran, Science **340**, 1545 (2013).
5. H. Huang, G. Xie, Y. Yan, N. Ahmed, Y. Ren, Y. Yue, D. Rogawski, M. J. Willner, B. I. Erkmen, K. M. Birnbaum, S. J. Dolinar, M. P. J. Lavery, M. J. Padgett, M. Tur, and A. E. Willner, Opt. Lett. **39**, 197 (2014).
6. Y. Li, H. Yang, J. Liu, L. Gong, Y. Sheng, W. Cheng, and S. Zhao, Chin. Opt. Lett. **11**, 021104 (2013).
7. Y. Zhang, M. Tang, and C. Tao, Chin. Opt. Lett. **3**, 559 (2005).
8. N. Bozinovic, S. Golowich, P. Kristensen, and S. Ramachandran, Opt. Lett. **37**, 2451 (2012).
9. Y. Yue, Y. Yan, N. Ahmed, J.-Y. Yang, L. Zhang, Y. Ren, H. Huang, K. M. Birnbaum, B. I. Erkmen, S. Dolinar, M. Tur, and A. E. Willner, IEEE Photon. J. **4**, 535 (2012).
10. S. Li and J. Wang, IEEE Photon. J. **5**, 7101007 (2013).
11. C. N. Alexeyev and M. A. Yavorsky, J. Opt. A **9**, 6 (2007).
12. C. N. Alexeyev and M. A. Yavorsky, J. Opt. A **6**, 824 (2004).
13. C. N. Alexeyev, A. V. Volyar, and M. A. Yavorsky, J. Opt. A **8**, L5 (2006).
14. Y. Yan, J. Wang, L. Zhang, J.-Y. Yang, I. M. Fazal, N. Ahmed, B. Shamee, A. E. Willner, K. Birnbaum, and S. Dolinar, Opt. Lett. **36**, 4269 (2011).
15. Y. Yan, L. Zhang, J. Wang, J. Yang, I. M. Fazal, N. Ahmed, A. E. Willner, and S. J. Dolinar, Opt. Lett. **37**, 3294 (2012).
16. Y. Yan, Y. Yue, H. Huang, J.-Y. Yang, M. R. Chitgarha, N. Ahmed, M. Tur, S. J. Dolinar, and A. E. Willner, Opt. Lett. **37**, 3645 (2012).
17. B. C. Sarkar, P. K. Choudhury, and T. Yoshino, Microwave Opt. Technol. Lett. **31**, 435 (2001).
18. J. Marcou and S. Février, Microwave Opt. Technol. Lett. **38**, 249 (2003).
19. C. N. Alexeyev, A. V. Volyar, and M. A. Yavorsky, J. Opt. A **9**, 387 (2007).
20. W. Snyder and J. Love, *Optical Waveguide Theory* (Chapman & Hall, 1983).
21. S. Ramachandran, P. Kristensen, and M. F. Yan, Opt. Lett. **34**, 2525 (2009).
22. S. Lang, *Linear Algebra* (Springer, 2004).